Model Representation of Secondary Organic Aerosol in CMAQv4.7

Annmarie G. Carlton*, Prakash V. Bhave*, Sergey L. Napelenok, Edward O. Edney, Golam Sarwar, Robert W. Pinder, George A. Pouliot, Marc Houyoux

U.S. Environmental Protection Agency, Research Triangle Park, Durham, NC 27711

*To whom correspondence should be addressed: carlton.annmarie@epa.gov, bhave.prakash@epa.gov

Revised text submitted to Environmental Science and Technology

ABSTRACT

Numerous scientific upgrades to the representation of secondary organic aerosol (SOA) are incorporated into the Community Multi-scale Air Quality (CMAQ) modeling system. Additions include several recently-identified SOA precursors: benzene, isoprene, and sesquiterpenes; and pathways: in-cloud oxidation of glyoxal and methylglyoxal, particle-phase oligomerization, and acid enhancement of isoprene SOA. NO_x-dependent aromatic SOA yields are also added along with new empirical measurements of the enthalpies of vaporization and organic mass-to-carbon ratios. For the first time, these SOA precursors, pathways and empirical parameters are included simultaneously in an air quality model for an annual simulation spanning the continental U.S. Year-long comparisons of CMAQ-modeled secondary organic carbon (OC_{sec}) with semi-empirical estimates screened from 165 routine monitoring sites across the U.S. indicate the new SOA module substantially improves model performance. The new SOA module better represents seasonal and regional patterns in biogenic SOA. The most notable improvement occurs in the central and southeastern U.S. where the regionally-averaged temporal correlations (r) between modeled and observationally-estimated OC_{sec} increase from -0.5 to 0.8 and -0.3 to 0.8, respectively, when the new SOA module is employed. Wintertime OC_{sec} results improve in all regions of the continental U.S.

INTRODUCTION

The simplistic treatment of secondary organic aerosol (SOA) is a source of considerable uncertainty in air quality model predictions [1]. SOA typically forms in the atmosphere when organic gases react with oxidants (e.g., O_3, OH, NO_3) and form low-volatility products that can be absorbed into the organic fraction of particulate matter (PM). In the U.S., secondary formation typically accounts for 50% of particulate organic carbon (OC) in summer and 20% in

winter [2]. Regional air quality models consistently underestimate ground-level fine PM in the summer at both urban and rural locations, primarily a result of errors in organic PM [3-7]. Conversely, wintertime OC is often overestimated [8, 9] due, in part, to SOA formulations that employ overestimated enthalpy of vaporization (ΔH_{vap}) values [10]. In addition, models predict little to no anthropogenic SOA [11, 12] though it is observed in the atmosphere (e.g., [13, 14]). These biases persist even when detailed SOA mechanisms and partitioning schemes are employed [15], suggesting that the current SOA treatment typically used in atmospheric models is incomplete and requires revision [16].

New findings indicate that several atmospherically-important SOA precursors and formation pathways are not widely incorporated in air quality models. For example, isoprene, sesquiterpenes, and benzene have recently been recognized as SOA precursors [17-19] that contribute substantially to ambient organic PM [20-24]. There is increasing evidence that SOA formation is influenced by the abundance of NO_x [18, 25-29], the acidity of seed particles [30-32], and the extent of atmospheric aging [33-35]. In addition to gas-phase oxidation of organic compounds, it is becoming well-established that SOA can form through aqueous oxidation processes [36-38]. Finally, mounting evidence from laboratory and field measurements indicates that atmospheric SOA exhibits very low volatility (e.g., LV-OOA) [28, 35], yet atmospheric models typically treat all SOA as semi-volatile compounds that partition reversibly between the gas and particulate phases.

CMAQ is among the most widely used air quality models, with 2000^{+} registered users in 90 different countries (www.cmaq-model.org). The U.S.EPA, as well as State and local governments, use CMAQ for regulatory applications (e.g., [39]) and the National Oceanic and Atmospheric Administration (NOAA) employs CMAQ for routine air quality forecasting [40].

Given the widespread use of CMAQ, it is important that its algorithms reflect scientific knowledge that is accepted across the research community. The last major update to the SOA treatment in a public version of CMAQ was in 2003 as part of version 4.3. Since then, researchers have used the CMAQ modeling framework to explore the importance of various SOA formation pathways and parameterizations (e.g., [1, 11, 15, 24, 41, 42]). Meanwhile, a number of SOA formation mechanisms proposed by other researchers were assessed in EPA's smog chamber facilities (e.g., [21, 31, 43-45] and a tracer-based method for estimating the contributions of different sources to ambient SOA was developed [14].

The purpose of this paper is to describe updates to the SOA treatment in version 4.7 of the CMAQ model (CMAQv4.7) and document the impact of those updates on a year-long model simulation spanning the continental United States. Principal objectives of CMAQv4.7 are to simulate all major SOA formation processes that are supported by peer-reviewed laboratory studies and all major sources of SOA that have been identified in field samples, without adding substantially to the computational burden of CMAQv4.6. Given the rate at which new knowledge about SOA is being generated in the literature, it is not possible for models to keep pace with every new finding. The SOA treatment described in the present study reflects the state of scientific knowledge as of August 2007. After extensive testing, the new model formulation was released to the public in December 2008 as part of CMAQv4.7. Other major improvements to CMAQv4.7 include an updated N_2O_5 hydrolysis parameterization, dynamic mass transfer for coarse-mode aerosol, revisions to the cloud model and new photolysis modeling options [7].

MODEL DESCRIPTION

The SOA treatment in CMAQv4.3 through v4.6 has been described elsewhere (Section S-1, Figure S1). In those model versions, SOA was formed exclusively via gas-phase oxidation of

monoterpenes, alkyl-substituted single-ring aromatics, cresol, and long alkanes, by free radicals (OH, NO_3, $O(^3P)$) and O_3. The semi-volatile products of these oxidation reactions were subsequently absorbed into an organic particulate phase [46, 47] and their gas/particle partitioning behavior was parameterized with a strong temperature dependence (ΔH_{vap}= 156 kJ mol^{-1}). A detailed description of the SOA treatment in previous CMAQ versions is provided in Section S1, along with the governing equations for modeling semi-volatile partitioning.

In CMAQv4.7, SOA is produced from an expanded list of precursors (Table 1) and can be formed via both gas- and aqueous-phase oxidation processes, as well as aerosol-phase reactions. Seven of the 19 secondary organic PM species are treated as non-volatile (dark-shaded rectangles in Figure 1). The 12 remaining species are semi-volatile and have ΔH_{vap} values reduced in accordance with recent experimental data [48]. Effective saturation concentrations (c*) at 298 K are derived from laboratory data using the new ΔH_{vap} values and assuming a representative chamber temperature (Table 1 footnote).

Semi-volatile SOA

In CMAQv4.7, seven organic species (shown along the left edge of Figure 1) may be oxidized in the gas phase to form semi-volatile products. The stoichiometric yields (α) and partitioning parameters (c*, ΔH_{vap}) of these products are provided in Table 1. Whereas previous versions of CMAQ treated monoterpenes as the only biogenic precursor of SOA, CMAQv4.7 includes SOA formation from isoprene, monoterpenes, and sesquiterpenes. Isoprene SOA is formed exclusively via oxidation by OH. Its yield and partitioning behavior are modeled according to the two-product parameterization of Henze and Seinfeld [22], based on the low-NO_x laboratory experiments of Kroll et al. [18]. As in previous versions of CMAQ, SOA parameters for monoterpenes are based on the daylight experiments of Griffin et al. [49]. Yields and

93 partitioning parameters for five different monoterpenes are lumped together using U.S.
94 emissions-based weighting factors (see Table S1) and the methodology of Bian and Bowman
95 [50]. In CMAQv4.7, the mass-based yields (α_{TRP1} and α_{TRP2}) and partitioning parameters (c^*_{TRP1},
96 c^*_{TRP2}) are corrected to replace the original assumption of unit density [49] with more recent
97 experimental data (Section S1). SOA from sesquiterpenes is parameterized in an analogous
98 fashion (i.e., experimental data of Griffin et al. [49], emissions-based lumping [50], and density
99 correction), but only one semi-volatile product (SV_SQT) is required to fit the laboratory data
100 [49]. One of the most consequential updates in CMAQv4.7 is the reduction of ΔH_{vap} from 156 kJ
101 mol^{-1} to 40 kJ mol^{-1} for all biogenic SOA species, based on recent chamber measurements of α-
102 pinene SOA [48]. The organic mass-to-carbon ratios (OM/OC) in Table 1 are obtained from
103 laboratory measurements [14] and used to estimate the molar masses (*M*) of each semi-volatile
104 product for the absorptive partitioning calculations.
105 The formation of semi-volatile SOA from anthropogenic organic gases is depicted in the
106 upper-left portion of Figure 1 and parameters are given in Table 1. Like previous versions of
107 CMAQ, long alkanes (~8 carbon atoms) oxidize to yield one semi-volatile product (SV_ALK)
108 that is parameterized by Strader et al. [51] based on early measurements of Grosjean and
109 Seinfeld [52]. Due to the lack of experimental data at the time of this model update, we
110 arbitrarily assign SV_ALK the same ΔH_{vap} as our biogenic oxidation products (i.e., 40 kJ mol^{-1})
111 and a molar mass of 150 g mol^{-1}. In previous CMAQ model versions, SOA formation from
112 aromatic compounds was parameterized based on the laboratory data of Odum et al. [53] by
113 assuming that a single reaction with the OH radical would produce semi-volatile products. In
114 CMAQv4.7, α and c* values for the semi-volatile aromatic reaction products are taken from
115 newer laboratory data [28] and these products are formed via a 2-step process: initial reaction

with OH produces aromatic peroxy radicals and subsequent reaction of the peroxy radicals with NO yields semi-volatile organic nitrates [23]. This treatment is applied to high-yield aromatics (based on laboratory data for toluene), low-yield aromatics (based on *m*-xylene data), and benzene. The OM/OC ratio of 2.0 for all six semi-volatile aromatic reaction products is taken from laboratory measurements of toluene SOA [14]. For the low-yield aromatic products (SV_XYL1 and SV_XYL2), ΔH_{vap} is taken from laboratory irradiations of *m*-xylene and 1,3,5-trimethylbenzene (J.H. Offenberg, personal communication). The ΔH_{vap} value for SV_TOL1 and SV_TOL2 (18 kJ mol^{-1}) is from the upper end of the range for toluene (13.8 to 17.5 kJ mol^{-1}) [48] and is also applied to the benzene products (SV_BNZ1 and SV_BNZ2). Our final update to the semi-volatile SOA treatment in CMAQv4.7 is the removal of cresol as an explicit SOA precursor. Any SOA formed from cresol is likely counted in the toluene SOA parameterization described above, because cresol is a product of toluene oxidation.

Non-Volatile SOA

A major enhancement to the SOA treatment in CMAQv4.7 is the inclusion of non-volatile SOA species, which are depicted as dark-shaded rectangles in Figure 1. Unlike the semi-volatile SOA described above, these species do not partition back to the gas phase. Four types of non-volatile SOA are included in CMAQv4.7 (see bottom of Table 1): 1) low-NO_x aromatic SOA, 2) acid-enhanced isoprene SOA, 3) oligomers formed through particle-phase reactions and 4) SOA from aqueous-phase oxidation.

Under low-NO_x conditions, aromatic peroxy radicals react preferentially with HO_2 (instead of NO) to produce non-volatile SOA [28]. Although ground-level HO_2 mixing ratios in CMAQ are 1 – 2 orders of magnitude smaller than NO across the remote continental U.S. and over 1000 times smaller than NO in urban areas, the low HO_2 abundance is slightly compensated

by its fast reaction rate with aromatic peroxy radicals (50% faster than the rate of RO_2+NO at 35°C and 150% faster at -10°C; see Table S2). Moreover, the stoichiometric yields of non-volatile products are substantially larger than those of the semi-volatile products (see Table 1). Combining the faster reaction rates and larger yields with the fact that the RO_2+HO_2 reaction products reside entirely within the particle phase, we expect non-volatile aromatic SOA to rival the abundance of the semi-volatile species described above (ATOL1, ATOL2, AXYL1, etc.) [23].

Although several laboratory studies have demonstrated that organic PM production from isoprene is enhanced relative to pH-neutral conditions [21, 30, 31], only Surratt and co-workers include a parameterization of the impact of acidity. In their study, an enhancement factor, k_{acid} = 0.00361 m^3 $nmol^{-1}$, is calculated from Figure 1 of reference [31] by normalizing the laboratory-derived slope (0.0389 μgC $nmol^{-1}$) by the intercept term (10.733 μgC m^{-3}) shown in that figure. Acidity is parameterized using the particle-phase hydrogen ion concentration in air (H^+ nmol m^{-3} air), which we estimate by subtracting the molar concentration of fine-particle cations (ammonium and sodium) from the equivalent concentration of anions (nitrate, chloride and twice the sulfate) and we constrain the applied acidity within the range of experimental data ($0 \leq [H^+] \leq 530$ nmol m^{-3}) [31]. The additional secondary carbon due to particle acidity is treated as a non-volatile species in CMAQ and is calculated by multiplying k_{acid} by the isoprene SOC formed via semi-volatile partitioning, with appropriate measures to ensure mass conservation.

All semi-volatile organic PM species in the model undergo condensed-phase oligomerization reactions that produce non-volatile products by a first order rate, $k_{olig} = 9.6\times10^{-6}$ sec^{-1}, corresponding to a 20-hour half life [11, 33]. The oligomers originating from biogenic gases (AOLGB) are tracked separately from those originating from anthropogenic gases

(AOLGA). The OM/OC ratio for oligomers (2.1) is based on a recommended value for non-urban areas [54].

The final non-volatile species in CMAQv4.7 (AORGC) forms from aqueous-phase oxidation of glyoxal and methylglyoxal by the hydroxyl radical (·OH). These constituents partition into cloud and fog water according to Henry's Law and low-volatility reaction products remain in the particle phase after the droplets evaporate. This treatment is depicted on the right side of Figure 1 and has been described in detail in a separate publication [42]. The OM/OC ratio (2.0) is estimated from laboratory experiments [55].

Gas-phase Chemistry

CMAQ is fully compatible with two chemical mechanisms: a recently-updated Carbon Bond mechanism (CB05) [56] and the 1999 Statewide Air Pollution Research Center mechanism (SAPRC99) [57]. To each mechanism, we added ten reactions and modified several existing reactions to accommodate the new SOA treatment in CMAQv4.7 (see Tables S2 and S3). Neither mechanism contains a sesquiterpene species, so three of our new reactions simulate the oxidation of sesquiterpenes by O_3, OH, and NO_3. Due to the large uncertainties in sesquiterpene emissions and in the rates and product distribution of the various reactions that may follow the initial oxidation, we incorporated only their first-generation decay in a manner that does not consume oxidants (e.g., SESQ + O_3 → SV_SQT + O_3) or affect CMAQ predictions of O_3 and other gases. Neither CB05 nor SAPRC99 treat benzene explicitly, so we added three reactions to simulate the oxidation of benzene by OH and subsequent reactions of the benzene peroxy radical with NO and HO_2. Finally, we added four reactions to simulate the interactions of high- and low-yield aromatic peroxy radicals with NO and HO_2. See Section S-2 for a complete description of these mechanistic changes.

Deposition

Dry and wet deposition of all 19 particle-phase organic species mimic the treatment applied to inorganic PM species in previous CMAQ versions [58, 59]. Note that deposition is the only removal mechanism for non-volatile SOA. For the semi-volatile organic gases (i.e., SV species in Figure 1), wet deposition is simulated using adipic acid as a surrogate and dry deposition velocities are copied from acetic acid. Critical properties for these processes are Henry's Law constant, molecular weight, diffusivity and relative reactivity.

METHODS

Model Simulations

Two CMAQ simulations of the 2003 calendar year are conducted on a 36-km grid that spans the continental U.S. from the Earth's surface to a 100mb altitude (112 rows × 148 columns × 14 layers = 232 064 computational cells). Both simulations are driven by identical weather fields from the MM5 meteorological model [60]. The first simulation uses the publicly-available CMAQv4.6 source code with SAPRC99 chemical mechanism and Rosenbrock solver, plus some minor code changes described. The second simulation, referred to hereafter as CMAQv4.6s, uses the same code except the SOA treatment is copied from CMAQv4.7. Source code for the latter simulation is available from the authors upon request. We purposely do not apply the full CMAQv4.7 model for the second simulation because v4.7 contains several scientific updates unrelated to SOA [7] and our objective is to isolate only the impacts of our new SOA treatment on CMAQ model performance. In addition to the two annual simulations, three 21-day simulations (August 15 – September 4, 2003) are conducted with each model version (v4.6 and v4.6s) to examine the sensitivity of modeled SOA to anthropogenic emissions of nitrogen oxides (NO_x), volatile organic compounds (VOC), and primary OC (OC_{pri}).

208 *Boundary conditions*

209 For the CMAQv4.6s simulations, concentrations of anthropogenic SOA species at the
210 domain boundaries are obtained directly from the global modeling results of Henze et al. [23]
211 and biogenic SOA species are obtained from Chung and Seinfeld [61] and Liao et al. [5].
212 Boundary values for SOA species that were not explicitly treated in those studies (e.g., AALK,
213 ASQT, AOLGA, AOLGB) are scaled from the available explicit values using ratios observed in
214 CMAQ simulations near the borders of the continental U.S. modeling domain. Temperature-
215 corrected concentrations of semi-volatile gases are calculated at the boundaries as a fractional
216 ratio of c* and the POC concentration is approximated as 0.150 μg m^{-3} [61]. The vertical
217 distribution of species, for which additional information was not available, is scaled (exponential
218 decay) from surface-level concentrations [62]. See Section S3 for a complete description of the
219 revised CMAQ boundary conditions.

220 *Emissions*

221 For all simulations, anthropogenic emissions are taken from the EPA's 2002 National
222 Emissions Inventory (NEI). Emissions of biogenic species are computed using the Biogenic
223 Emission Inventory System (BEIS), which we updated to incorporate sesquiterpene emissions.
224 Sesquiterpenes are lumped into a single compound class using available measurements for α-
225 farnasene, β –caryophyllene, and various other sesquiterpenes. Basal emission rates (BER) are
226 derived from the EF-S06 data set tabulated by Sakulyanontvittaya et al. [24]. Dividing each
227 emission factor by the corresponding biomass density from that study, we obtain BER of 0.175,
228 0.1084, 0.0552, and 0.2036 μg g_{dry}^{-1} hr^{-1}, for broadleaf trees, needle-leaf trees, shrubs and bushes,
229 and grasses and crops, respectively. Each of the 230 tree species in BEIS is mapped to one of

these BER except Loblolly pine, for which 0.3 μg g_{dry}^{-1} hr^{-1} is used [63]. All BER are modulated based on the 2-meter air temperature in each grid cell (T, K),

$$ER = BER * e^{0.17(T-303)} \quad (1)$$

to obtain a temporally- and grid-specific emission rate (ER). The factor of 0.17 is based on outdoor measurements [64].

Model Evaluation

CMAQ model performance is evaluated against semi-empirical estimates of secondary organic carbon (OC_{sec}) by the procedure of Yu et al. [2].

$$OC_{sec} = OC_{obs} - \left[\min\left(OC_{obs}, \left(\frac{OC}{EC}\right)_{pri} \times EC_{obs} \right) \right] \quad (2)$$

The *obs* subscript indicates concentrations observed at Interagency Monitoring of PROtected Visual Environments (IMPROVE) (http://vista.cira.colostate.edu/improve) and Southeastern Aerosol Research and CHaracterization (SEARCH) (http://www.atmospheric-research.com/public/) network sites. $(OC/EC)_{pri}$ is a ratio calculated from CMAQ outputs of OC_{pri} and EC, reflecting the mixture of primary sources impacting a given site at the time when each sample was collected. Model-predicted ratios were assessed at all 165 monitoring sites by the procedure described in Yu et al. [2], and 97 sites were selected for the subsequent model evaluation of OC_{sec} (Figure S2).

In CMAQv4.6, OC_{sec} is calculated from Equation (1) of reference [9]. In CMAQv4.6s, it is the sum of all 19 SOA species divided by the OM/OC ratios listed in Table 1. Hourly OC_{sec} concentrations from each annual simulation are paired in space with the semi-empirical estimates screened from 165 monitoring sites across the U.S. (Figure S2) and temporally averaged to match the 24-hour sampling schedule of each network.

RESULTS AND DISCUSSION

The diversity of SOA species in CMAQv4.6s is substantially more complex than in previous model versions, allowing for assignment of SOA mass to individual VOC precursors. With CMAQv4.6, SOA derived from monoterpenes comprises most of the predicted OC_{sec} (Figure 2) and anthropogenic precursors contribute a small amount to a single anthropogenic SOA species. With CMAQv4.6s, biogenic SOA still dominates OC_{sec} predictions but there are four species that can be assigned to three VOC precursors and two different formation processes. Similarly, in v4.6s there are five anthropogenic SOA species traceable to four VOC precursors and predictions increase as a result of the additional species and formation pathways [7], (Figure S-3).

The seasonal pattern for biogenic SOA mass predictions improves with the new SOA mechanism [7], (Figure S-4). However, the magnitude of predicted SOA mass decreases (Figures 2), despite the addition of two biogenic precursors (isoprene and sesquiterpens) and an additional formation pathway (oligomerization). This result largely arises from the assigned enthalpy of vaporization (ΔH_{vap}) value of 156 kJ mol^{-1} in CMAQv4.6 for biogenic SOA, compared to the 40 kJ mol^{-1} value in CMAQv4.6s. The change to a lower ΔH_{vap} value causes less semivolatile material to partition into the particle phase, and in general, less biogenic SOA is predicted as a consequence. This very large effect is evidenced by comparing the v4.6 biogenic OC_{sec} (gray in Figure 2a) (which originates entirely from monoterpenes) with OC_{sec} from monoterpenes in v4.6s (light green in Figure 2b).

Comparison with semi-empirical OC_{sec} estimates

CMAQv4.6s simulations demonstrate better agreement with semi-empirical OC_{sec} estimates than v4.6 (Figure 2). When averaged by month across 97 sites, temporal correlation (r)

between the modeled and semi-empirical OC_{sec} concentrations improves from 0.54 in CMAQv4.6 to 0.86using CMAQv4.6s. This correlation also improves in individual regions of the U.S., most notably in the central states and Southeast, where CMAQv4.6 exhibits a negative correlation with the semi-empirical estimates (-0.4 and -0.3, respectively) and v4.6s exhibits a large positive correlation (0.8 and 0.8) (Figures S-5 and S-6). In addition to the improved correlation, we note that v4.6s exhibits a slope closer to unity and an intercept closer to zero than v4.6 (see Figure 2).

The improved spatial and temporal trends in biogenic SOA, which dominates predicted OC_{sec} concentrations in both simulations (Figure 2), drives the enhanced model performance. In contrast to CMAQv4.6, the revised SOA treatment (v4.6s) produces summertime maxima for OC_{sec} in all regions, consistent with the observational estimates (compare Figures S-5 and S-6). In addition, the wintertime (December – March) overestimates of OC_{sec} that were evident in CMAQ v4.6 are eliminated by the new SOA treatment (Figure 2).

Emissions Sensitivities

Our updated SOA treatment also affects CMAQ predictions of how ambient SOA might respond to future NO_x, VOC, and OC_{pri} emission controls. To evaluate these effects, three 21-day simulations (August 15 – September 4, 2003) were conducted with v4.6 and v4.6s in which all controllable emissions of NO_x, VOC or OC_{pri} were removed. Relative to v4.6, CMAQv4.6s predictions of SOA from anthropogenic VOC exhibit diminished sensitivity to NO_x and OC_{pri} (Figure 3a). Note that in this context anthropogenic VOC refers to alkanes and aromatic compounds, for which some uncontrollable sources (e.g., wildfires) exist [65]. The diminished sensitivities in v4.6s arise from low-NO_x aromatic oxidation pathways that produce non-volatile SOA with high stochiometeric yield, and particle-phase oligomerization pathways that are

independent of OC_{pri} concentrations. In contrast, v4.6s predictions of SOA from biogenic VOC exhibit heightened sensitivity to OC_{pri} emissions (Figure 3b). This increased sensitivity arises from the v4.6s addition of highly-reactive sesquiterpenes, whose SOA-forming potential is limited only by the amount of available absorbing organic mass [65]. Total SOA predictions in v4.6s also exhibit heightened sensitivity to VOC emission controls (Figure 3c) due to the larger contribution of anthropogenic VOCs to the total SOA mass.

Future Model Development

The SOA mechanism in CMAQ includes several new SOA precursors and formation pathways, reflecting the state of scientific knowledge as of August 2007. Predicted trends and patterns for OC_{sec} are better with the new mechanism, especially for biogenic products. However, a substantial negative bias in summertime OC_{sec} persists, suggesting that uncharacterized SOA sources exist and/or current modeling approaches are insufficient (e.g., [35]). Future model upgrades may require the addition of more SOA precursors and pathways [66], and will be guided by diagnostic model evaluations against organic tracer data [45].

ACKNOWLEDGEMENTS

This work is the result of a large collaboration across EPA involving a variety of groups, namely AMAD, HEASD, NRMRL, OAQPS, OTAQ and NCER. The authors acknowledge helpful contributions from Kristen Foley, Heather Simon, Nancy Hwang, Charles Chang, Lucille Bender and Ruen Tang. We acknowledge Rob Griffin for verifying data and methods used in his 1999 JGR article and Rohit Mathur and Bill Benjey for administrative support. Bonyoung Koo, Greg Yarwood, Ralph Morris provided helpful discussions during the development of new SOA module.

DISCLAIMER

Although this paper has been reviewed by EPA and approved for publication, it does not necessarily reflect EPA's policies or views.

References

1. Pun, B. K.; Wu, S.-Y.; Seigneur, C.; Seinfeld, J. H.; Griffin, R. J.; Pandis, S. N. Uncertainties in modeling secondary organic aerosols: three dimensional modeling studies in Nashville/western Tennessee. *Environ. Sci. Technol.* **2003**, *37*, 3647-3661.
2. Yu, S.; Bhave, P. V.; Dennis, R. L.; Mathur, R. Seasonal and regional variations of primary and secondary organic aerosols over the continental United States: semi-empirical estimates and model evaluation. *Environ. Sci. Technol.* **2007**, *41*, 4690-4697.
3. Tesche, T. W.; Morris, R.; Tonnesen, G.; McNally, D.; Boylan, J.; Brewer, P. CMAQ/CAM_x annual 2002 performance evaluation over the eastern US. *Atmos. Environ.***2006**, *40*, 4906-4919.
4. McKeen, S.; et al., Evaluation of several $PM_{2.5}$ forecast models using data collected during the ICARTT/NEAQS 2004 field study. *J. Geophys. Res.* **2007**, *112*, D10S20.
5. Liao, H.; Henze, D. K.; Seinfeld, J. H.; Wu, S. L.; Mickley, L. J. Biogenic secondary organic aerosol over the United States: Comparison of climatological simulations with observations. *J. Geophys. Res.* **2007**, *112*, D06201.
6. Yu, S.; et al., Evaluation of real-time $PM_{2.5}$ forecasts and process analysis for $PM_{2.5}$ formation over the eastern United States using the Eta-CMAQ forecast model during the 2004 ICARTT study. *J. Geophys. Res.* **2008**, *113*, D06204.
7. Foley, K. M.; et al., Incremental testing of the Community Multiscale Air Quality (CMAQ) modeling system version 4.7. *Geosci. Model Dev.* **2010**, *3*, 205-226.
8. Mathur, R.; Yu, S.; Kang, D.; Schere, K. L. Assessment of the wintertime performance of developmental particulate matter forecasts with the Eta-Community Multiscale Air Quality modeling system. *J. Geophys. Res.* **2008**, *113*, D02303.
9. Appel, K. W.; Bhave, P. V.; Gilliland, A. B.; Sarwar, G.; Roselle, S. J. Evaluation of the Community Multiscale Air Quality (CMAQ) model version 4.5: sensitivities impacting model performance; Part II - particulate mater. *Atmos. Environ.* **2008**, *42*, 6057-6066.
10. Pun, B. K.; Seigneur, C. Organic aerosol spatial/temporal patterns: perspectives of measurements and model. *Environ. Sci. Technol.* **2008**, *42*, 7287-7293.
11. Morris, R. E.; Koo, B.; Guenther, A.; Yarwood, G.; McNally, D.; Tesche, T. W.; Tonnesen, G.; Boylan, J.; Brewer, P. Model sensitivity evaluation for organic carbon using two multi-pollutant air quality models that simulate regional haze in the southeastern United States. *Atmos. Environ.* **2006**, *40*, 4960-4972.
12. Simpson, D.; Yttri, K. E.; Klimont, Z.; Kupiainen, K.; Caseiro, A.; Gelencsér, A.; Pio, C.; Puxbaum, H.; Legrand, M. Modeling carbonaceous aerosol over Europe: analysis of the CARBOSOL and EMEP EC/OC campaigns. *J. Geophys. Res.* **2007**, *112*, D23S14.
13. Volkamer, R.; Jimenez, J. L.; San Martini, F.; Dzepina, K.; Zhang, Q.; Salcedo, D.; Molina, L. T.; Worsnop, D. R.; Molina, M. J. Secondary organic aerosol formation from anthropogenic air pollution: rapid and higher than expected. *Geophys. Res. Lett.* **2006**, *33*, L17811.
14. Kleindienst, T. E.; Jaoui, M.; Lewandowski, M.; Offenberg, J. H.; Lewis, C. W.; Bhave, P. V.; Edney, E. O. Estimates of the contributions of biogenic and anthropogenic hydrocarbons to secondary organic aerosol at a southeastern US location. *Atmos. Environ.* **2007**, *41*, 8288-8300.
15. Chen, J.; Mao, H.; Talbot, R. W.; Griffin, R. J. Application of the CACM and MPMPO modules using the CMAQ model for the eastern United States. *J. Geophys. Res.* **2006**, *111*, D23S25.
16. De Gouw, J. and Jimenez, J. L. Organic aerosols in the Earth's atmosphere. *Environ. Sci. Technol.* **2009**, *43*, 7614-7618.

17. Martin-Reviejo, M.; Wirtz, K. Is benzene a precursor for secondary organic aerosol? *Environ. Sci. Technol.* **2005**, *39*, 1045-1054.
18. Kroll, J. H.; Ng, N. L.; Murphy, S. M.; Flagan, R. C.; Seinfeld, J. H. Secondary organic aerosol formation from isoprene photooxidation. *Environ. Sci.Technol.* **2006**, *40*, 1869-1877.
19. Lee, A.; Goldstein, A. H.; Kroll, J. H.; Ng, N. L.; Varutbangkul, V.; Flagan, R. C.; Seinfeld, J. H. Gas-phase products and secondary aerosol yields from the photooxidation of 16 different terpenes. *J. Geophys. Res.* **2006**, *111*, D17305.
20. Claeys, M.; Graham, B.; Vas, G.; Wang, W.; Vermeylen, R.; Pashynska, V.; Cafmeyer, J.; Guyon, P.; Andreae, M. O.; Araxo, P.; Maenhaut, W. Formation of secondary organic aerosols through photooxidation of isoprene. *Science* **2004**, *303*, 1173-1176.
21. Edney, E. O.; Kleindienst, T. E.; Jaoui, M.; Lewandowski, M.; Offenberg, J. H.; Wang, W.; Claeys, M. Formation of 2-methyl tetrols and 2-methylglyceric acid in secondary organic aerosol from laboratory irradiated isoprene/NO_x/SO_2/air mixtures and their detection in ambient $PM_{2.5}$ samples collected in the eastern United States. *Atmos. Environ.* **2005**, *39*, 5281-5289.
22. Henze, D. K.; Seinfeld, J. H. Global secondary organic aerosol from isoprene oxidation. *Geophys. Res. Lett.* **2006**, *33*, L09812.
23. Henze, D. K.; Seinfeld, J. H.; Ng, N. L.; Kroll, J. H.; Fu, T.-M.; Jacob, D. J.; Heald, C. L. Global modeling of secondary organic aerosol formation from aromatic hydrocarbons: high- vs. low-yield pathways. *Atmos. Chem. Phys.* **2008**, *8*, 2405-2420.
24. Sakulyanontvittaya, T.; Guenther, A.; Helmig, D.; Milford, J.; Wiedinmyer, C. Secondary organic aerosol from sesquiterpene and monoterpene emissions in the United States. *Environ. Sci. Technol.* **2008**, *42*, 8784-8790.
25. Hatakeyama, S.; Izumi, K.; Fukuyama, T.; Akimoto, H.; Washida, N. Reactions of OH with α-pinene and β-pinene in air: estimate of global CO production from the atmospheric oxidation of terpenes. *J. Geophys. Res.* **1991**, *96*, 947-958.
26. Presto, A. A.; Huff Hartz, K. E.; Donahue, N. M. Secondary organic aerosol production from terpene ozonolysis. 2. Effect of NO_x concentration. *Environ. Sci. Technol.* **2005**, *39*, 7046-7054.
27. Song, C.; Na, K.; Cocker, D. R. Impact of the hydrocarbon to NO_x ratio on secondary organic aerosol formation. *Environ. Sci. Technol.* **2005**, *39*, 3143-3149.
28. Ng, N. L.; Kroll, J. H.; Chan, A. W. H.; Chhabra, P. S.; Flagan, R. C.; Seinfeld, J. H. Secondary organic aerosol formation from m-xylene, toluene, and benzene. *Atmos. Chem. Phys.* **2007**, *7*, 3909-3922.
29. Ng, N. L.; et al., Effect of NO_x level on secondary organic aerosol (SOA) formation from the photooxidation of terpenes. *Atmos. Chem. Phys.* **2007**, *7*, 5159-5174.
30. Jang, M.; Czoschke, N. M.; Lee, S.; Kamens, R. M. Heterogeneous atmospheric aerosol production by acid-catalyzed particle-phase reactions. *Science* **2002**, *298*, 814-817.
31. Surratt, J. D.; Lewandowski, M.; Offenberg, J. H.; Jaoui, M.; Kleindienst, T. E.; Edney, E. O.; Seinfeld, J. H. Effect of acidity on secondary organic aerosol formation from isoprene. *Environ. Sci. Technol.* **2007**, *41*, 5363-5369.
32. Offenberg, J. H.; Lewandowski, M.; Edney, E. O.; Kleindienst, T. E.; Jaoui, M. Influence of aerosol acidity on the formation of secondary organic aerosol from biogenic precursor hydrocarbons. *Environ. Sci. Technol.* **2009**, *43*, 7742-7747.
33. Kalberer, M.; Paulsen, D.; Sax, M.; Steinbacher, M.; Dommen, J.; Prevot, A. S. H.; Fisseha, R.; Weingartner, E.; Frankevich, V.; Zenobi, R.; Baltensperger, U. Identification of polymers as major components of atmospheric organic aerosols. *Science* **2004**, *303*, 1659-1662.
34. Rudich, Y.; Donahue, N. M.; Mentel, T. F. Aging of organic aerosol: Bridging the gap between laboratory and field studies. *Ann. Rev. Phys. Chem.* **2007**, *58*, 321-352.
35. Jimenez, J. L.; et al., Evolution of organic aerosols in the atmosphere. *Science* **2009**, *326*, 1525-1529.

36. Carlton, A. G.; Turpin, B. J.; Altieri, K. E.; Reff, A.; Seitzinger, S.; Lim, H.-J.; Ervens, B. Atmospheric oxalic acid and SOA production from glyoxal: results of aqueous photooxidation experiments. *Atmos. Environ.* **2007**, *41*, 7588-7602.
37. Volkamer, R.; Ziemann, P. J.; Molina, M. J. Secondary Organic Aerosol Formation from Acetylene (C_2H_2): seed effect on SOA yields due to organic photochemistry in the aerosol aqueous phase. *Atmos. Chem. Phys.* **2009**, *9*, 1907-1928.
38. El Haddad, I.; Liu, Y.; Nieto-Gligorovski, L.; Michaud, V.; Temime-Roussel, B.; Quivet, E.; Marchand, N.; Sellegri, K.; Monod, A. In-cloud processes of methacrolein under simulated conditions - Part 2: formation of secondary organic aerosol. *Atmos. Chem. Phys.* **2009**, *9*, 5107-5117.
39. U. S. EPA - OAQPS, Technical Support Document for the Proposed PM NAAQS Rule: Response Suface Modeling. Research Triangle Park, NC, Feb. **2006**; http://www.epa.gov/scram001/reports/pmnaaqs_tsd_rsm_all_021606.pdf.
40. Otte, T. L.; et al., Linking the Eta model with the Community Multiscale Air Quality (CMAQ) modeling system to build a national air quality forecasting system. *Weather Forecast.* **2005**, *20*, 367-384.
41. Zhang, Y.; Huang, J.-P.; Henze, D. K.; Seinfeld, J. H. Role of isoprene in secondary organic aerosol formation on a regional scale. *J. Geophys. Res.* **2007**, *112*, D20207.
42. Carlton, A. G.; Turpin, B. J.; Altieri, K. E.; Seitzinger, S. P.; Mathur, R.; Roselle, S. J.; Weber, R. J. CMAQ model performance enhanced when in-cloud SOA is included: comparisons of OC predictions with measurements. *Environ. Sci. Technol.* **2008**, *42*, 8798-8802.
43. Kleindienst, T. E.; Smith, D. F.; Li, W.; Edney, E. O.; Driscoll, D. J.; Speer, R. E.; Weathers, W. S. Secondary organic aerosol formation from the oxidation of aromatic hydrocarbons in the presence of dry submicron ammonium sulfate aerosol. *Atmos. Environ.* **1999**, *33*, 3669-3681.
44. Edney, E. O.; Driscoll, D. J.; Speer, R. E.; Weathers, W. S.; Kleindienst, T. E.; Li, W.; Smith, D. F. Impact of aerosol liquid water on secondary organic aerosol yields of irradiated toluene/propylene/NO_x/$(NH_4)_2$ SO4/air mixtures. *Atmos. Environ.* **2000**, *34*, 3907-3919.
45. Jaoui, M.; Edney, E. O.; Kleindienst, T. E.; Lewandowski, M.; Offenberg, J. H.; Surratt, J. D.; Seinfeld, J. H. Formation of secondary organic aerosol from irradiated α-pinene/toluene/NO_x mixtures and the effect of isoprene and sulfur dioxide. *J. Geophys. Res.* **2008**, *113*, D09303.
46. Pankow, J. An absorption model of gas/particle partitioning of organic compounds in the atmosphere. *Atmos. Environ.* **1994**, *28*, 185-188.
47. Odum, J. R.; Hoffmann, T.; Bowman, F.; Collins, D.; Flagan, R. C.; Seinfeld, J. H. Gas/particle partitioning and secondary organic aerosol yields. *Environ. Sci. Technol.* **1996**, *30*, 2580-2585.
48. Offenberg, J. H.; Kleindienst, T. E.; Jaoui, M.; Lewandowski, M.; Edney, E. O. Thermal properties of secondary organic aerosols. *Geophys. Res. Lett.* **2006**, *33*, L03816.
49. Griffin, R. J.; Cocker, D. R.; Flagan, R.C.; Seinfeld, J. H. Organic aerosol frormation from the oxidation of biogenic hydrocarbons. *J. Geophys. Res.* **1999**, 104, 3555-3567.
50. Bian, F.; Bowman, F. M. Theoretical method for lumping multicomponent secondary organic aerosol mixtures. *Environ. Sci. Technol.* **2002**, *36*, 2491-2497.
51. Strader, R.; Lurmann, F.; Pandis, S. N. Evaluation of secondary organic aerosol formation in winter. *Atmos. Environ.* **1999**, *33*, 4849-4863.
52. Grosjean, D. and Seinfeld, J. H. Parameterization of the formation potential of secondary organic aerosols. *Atmos. Environ.* **1989**, *23*, 1733-1747.
53. Odum, J. R.; Jungkamp, T. P. W.; Griffin, R. J.; Forstner, H. J. L.; Flagan, R. C.; Seinfeld, J. H.,Aromatics, reformulated gasoline, and atmospheric organic aerosol formation. *Environ. Sci. Technol.* **1997**, *31*, 1890-1897.

54. Turpin, B. J. and Lim, H.-J.,Species contributions to PM2.5 mass concentrations: Revisiting common assumptions for estimating organic mass. *Aerosol Sci. Technol.* **2001**, *35*, 602-610.
55. Altieri, K. E.; Seitzinger, S. P.; Carlton, A. G.; Turpin, B. J.; Klein, G. C.; Marshall, A. G. Oligomers formed through in-cloud methylglyoxal reactions: chemical composition, properties, and mechanisms investigated by ultra-high resolution FT-ICR mass spectrometry. *Atmos. Environ.* **2008**, *42*, 1476-1490.
56. Sarwar, G.; Luecken, D.; Yarwood, G.; Whitten, G. Z.; Carter, W. P. L. Impact of an updated carbon bond mechanism on predictions from the CMAQ modeling system: preliminary assessment. *J. Appl. Meteorol. Clim.* **2008**, *47*, 3-14.
57. Carter, W. P. L. *Implementation of the SAPRC-99 chemical mechanism into the Models-3 framework*; U.S. EPA: **2000**.
58. Binkowski, F. S.; Roselle, S. J. Models-3 Community Multiscale Air Quality (CMAQ) model aerosol component - 1. Model description. *J. Geophys. Res.* **2003**, *108*, (D6).
59. Bhave, P.; Nolte, C.; Pleim, J.; Schwede, D.; Roselle, S. Recent Developments in the CMAQ Modal Aerosol Model, 4th Annual Community Modeling and Analysis System Conference, Chapel Hill, NC, **2005**.
60. Grell, G. A.; Dudhia, J.; Stauffer, D. R. *A description of the fifth-genration Penn State-NCAR Mesoscale Model (MM5)*; NCAR Tech. Note NCAR/TN-398+STR; National Center for Atmospheric Research: Boulder, CO, **1994**; p 122.
61. Chung, S. H.; Seinfeld, J. H. Global distribution and climate forcing of carbonaceous aerosols. *J. Geophys. Res. - Atmos.* **2002**, *107*, 4407.
62. Seinfeld, J. H.; Pandis, S. N. *Atmospheric Chemistry and Physics*. John Wiley and Sons, Inc.: New York, **1998**.
63. Duhl, T. R.; Helmig, D.; Guenther, A. Sesquiterpene emissions from vegetation: a review. *Biogeosciences* **2008**, *5*, 761-777.
64. Helmig, D.; Ortega, J.; Duhl, T.; Tanner, D.; Guenther, A.; Harley, P.; Wiedinmyer, C.; Milford, J.; Sakulyanontvittaya, T. Sesquiterpene emissions from pine trees: identifications, emission rates and flux estimates for the contiguous United States. *Environ. Sci. Technol.* **2007**, *41*, 1545-1553.
65. Carlton, A. G.; Pinder, R. W.; Bhave, P. V.; Pouliot, G. A. To what extent can biogenic SOA be controlled? *Environ. Sci. Technol.* **2010**, *44*, 3376-3380.
66. Hallquist, M.; et al., The formation, properties and impact of secondary organic aerosol: current and emerging issues. *Atmos. Chem. Phys.* **2009**, *9*, 5155-5236.

Table 1. Parameters for CMAQ v4.7 SOA Module

Gaseous Precursor (model species)	Oxidants	semi-volatile products	α_i [f]	c^* [g] ($\mu g\ m^{-3}$)	ΔH_{vap} ($kJ\ mol^{-1}$)	SOA Species	M ($g\ mol^{-1}$)	OM/OC ratio
Semi-volatile SOA								
Isoprene (ISOP[a] or ISOPRENE[b])	$^{\cdot}OH$	SV_ISO1	0.232	116.01	40	AISO1	96	
		SV_ISO2	0.0288	0.617	40	AISO2	96	1.6
Monoterpenes (TERP[a] or TRP1[b])	$^{\cdot}OH$, $O(^3P)$[e], O_3, $^{\cdot}NO_3$	SV_TRP1	0.1393	14.792	40	ATRP1	168	
		SV_TRP2	0.4592	133.7297	40	ATRP2	168	1.4
Sesquiterpenes (SESQ[a,b])	O_3, $^{\cdot}OH$, $^{\cdot}NO_3$	SV_SQT	1.537	24.984	40	ASQT	378	2.1
Alkanes (ALK5[b])	$^{\cdot}OH$	SV_ALK	0.0718	0.02	40	AALK	150	1.56
High-yield aromatics (ARO1[a] or TOL[b])	$^{\cdot}OH$/NO	SV_TOL1	0.0758	2.326	18	ATOL1	168	
		SV_TOL2	0.1477	21.277	18	ATOL2	168	2.0
Low-yield aromatics (XYL[a] or ARO2[b])	$^{\cdot}OH$/NO	SV_XYL1	0.0386	1.314	32	AXYL1	192	
		SV_XYL2	0.1119	34.483	32	AXYL2	192	2.0
Benzene (BENZENE[a] or BENZ[b])	$^{\cdot}OH$/NO	SV_BNZ1	0.0942	0.302	18	ABNZ1	144	
		SV_BNZ2	1.162	111.11	18	ABNZ2	144	2.0
Non-volatile SOA								
High-yield aromatics[c]	$^{\cdot}OH$/$^{\cdot}HO_2$		0.471	[h]	[h]	ATOL3	168	2.0
Low-yield aromatics[c]	$^{\cdot}OH$/$^{\cdot}HO_2$		0.373	[h]	[h]	AXYL3	192	2.0
Benzene[c]	$^{\cdot}OH$/$^{\cdot}HO_2$		0.484	[h]	[h]	ABNZ3	144	2.0
Isoprene	H^+			[h]	[h]	AISO3	162	2.7

aged aerosol	time			[h]	[h]	AOLGA, AOLGB	176.4 252	2.1
Glyoxal, methylglyoxal GLY[a], MGLY[a b d]	·OH	0.04				AORGC	177	2.0

[a]indicates species name in CB05 gas-phase mechanism. Long alkanes and glyoxal are not modeled explicitly in CB05.
[b]indicates name in SAPRC99
[c]low-NO_x pathways. Mole-based α values reported by Ng et al. [28] are divided by the stoichiometric coefficients for peroxy radical products (taken from the SAPRC99 gas-phase chemical mechanism) to obtain the values tabulated here (see Section S-1 for details).
[d]When CMAQ is exercised with the CB05 mechanism, the Henry's Law constant for methylglyoxal is adjusted in the aqueous chemistry routine to the glyoxal value (because GLY is not an explicit species in CB05) to ensure that simulations employing SAPRC99 and CB05 provide similar predictions of AORGC at similar aqueous phase aldehyde concentrations.
[e]There is no $O(^3P)$ species in the CB05 gas-phase mechanism. When CB05 is employed TRP1 reacts with singlet O to form SOA.
[f]α_j are mass-based stoichiometric yields. Whereas the α values for monoterpene and sesquiterpene oxidation are adjusted upward by a factor of 1.3 (see text), no such correction was needed for the isoprene and aromatic yields because there is not sufficient laboratory data
[g]c* values are tabulated at 298 K, using the ΔH_{vap} values shown and assuming a representative chamber temperature (313 K for monoterpenes, 310 K for sesquiterpenes, 281.5 K for long alkanes, and no correction for the remaining experiments which were conducted between 293 – 298 K)
[h]For non-volatile SOA, c* and ΔH_{vap} values are not required in atmospheric models.

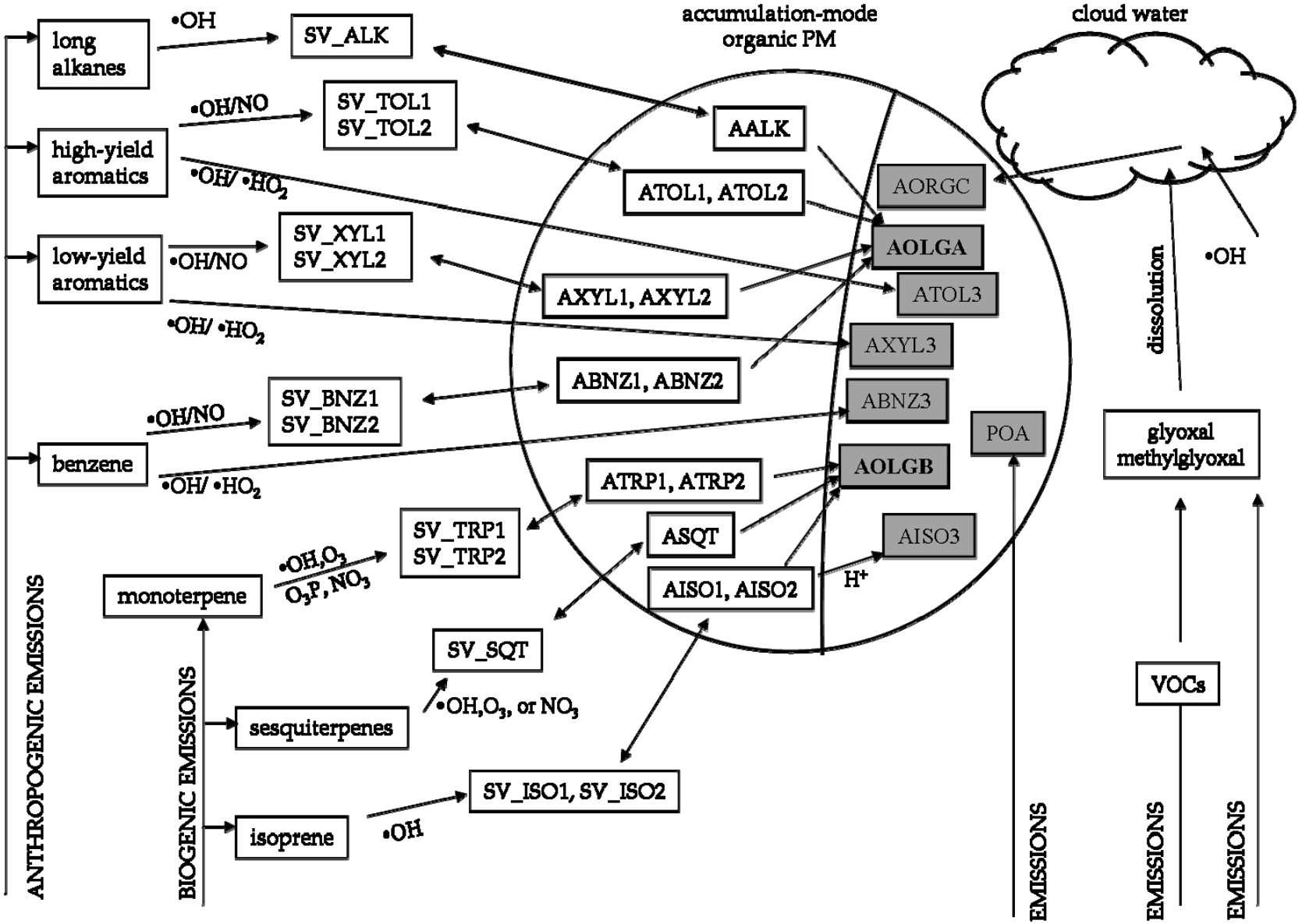

Figure 1. Schematic of CMAQv4.7s SOA module. Species inside the circle constitute the organic fine PM. Species in the dark shaded boxes are treated as non-volatile. Gas-phase oxidation pathways are depicted on the left and aqueous-phase oxidation is shown on the right. Double-headed arrows spanning the gas/particle interface represent the equilibrium partitioning of semi-volatile SOA species.

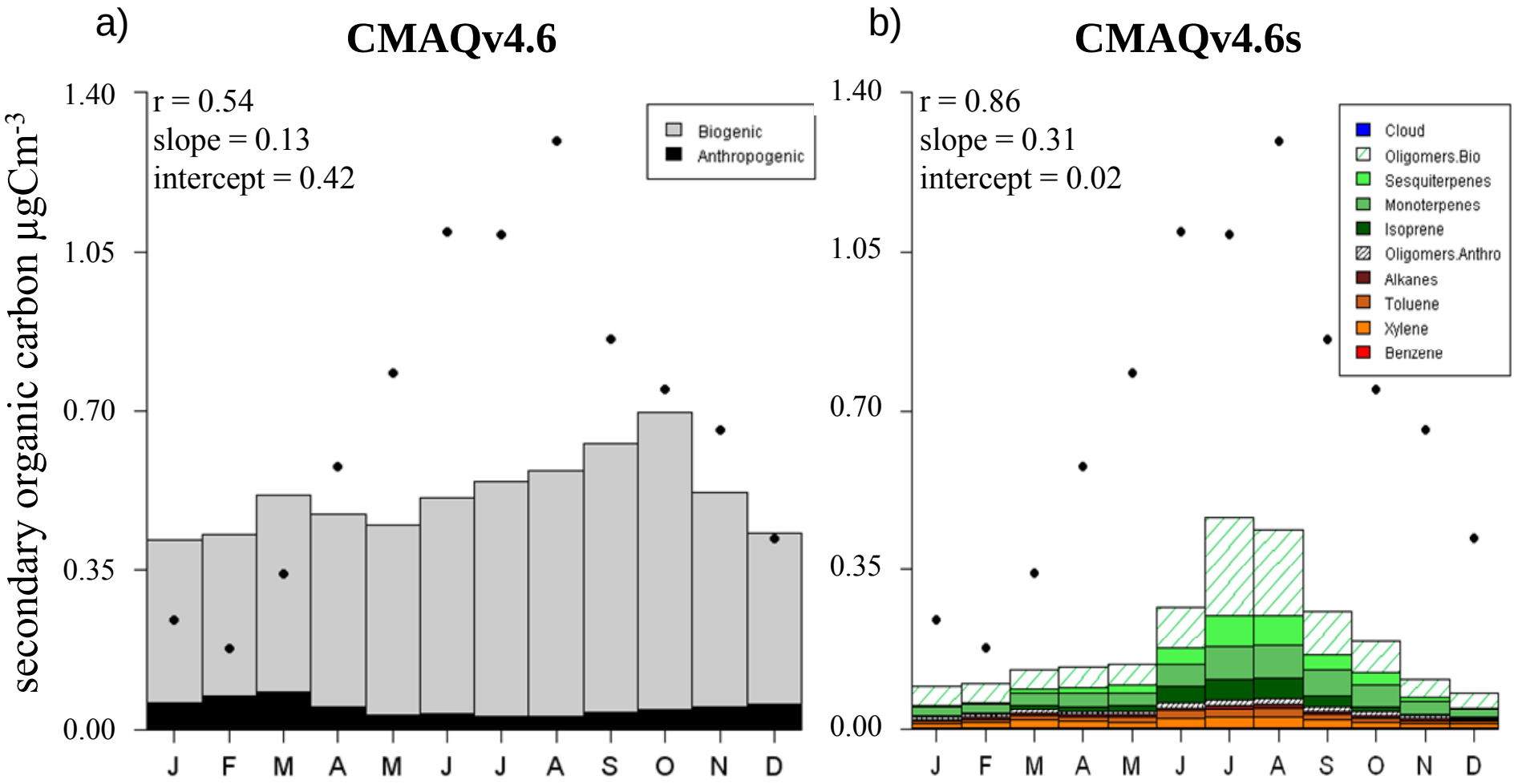

Figure 2. Seasonal profiles for CMAQ-predicted OC_{sec} (CMAQv4.6 on left, CMAQv4.6s on right) and semi-empirical estimates (•), averaged by month across the 97 sites shown in Figure S2.

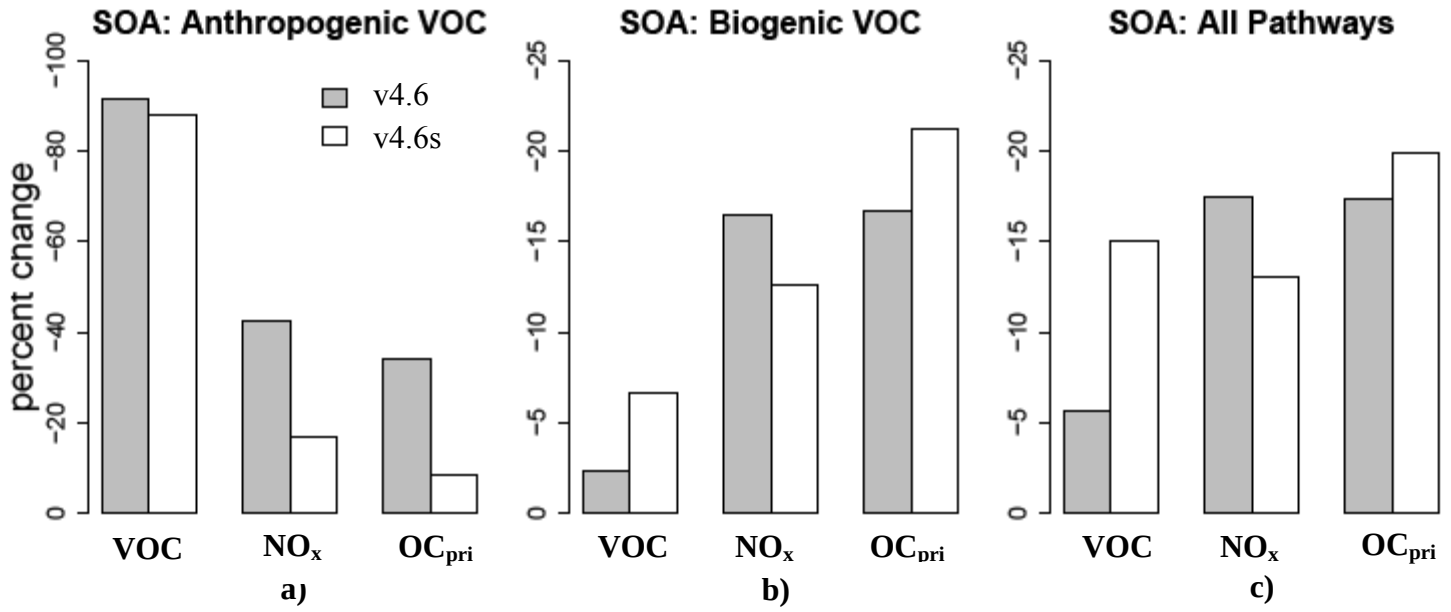

Figure 3. Sensitivity of SOA originating from anthropogenic VOC (a), biogenic VOC (b) and all pathways (c) to emission controls in summertime CMAQv4.6 and CMAQv4.6s simulations. Percent reductions are calculated from 21-day simulations using surface-level, domain-wide averages in which controllable emissions of VOCs, NO_x, and OC_{pri} are separately removed from the emission inputs. Note: SOA derived from glyoxal and methylglyoxal via cloud processing is counted in (c), but excluded from (a) and (b).